Proc. of the X Int. Conf. — Ion Implantation and other Applications of Ions and Electrons, Kazimierz Dolny 2014

Mechanisms of Carrier Transport in $Cu_x(SiO_2)_{1-x}$ Nanocomposites Manufactured by Ion-Beam Sputtering with Ar Ions

A. Fedotov[a], A. Mazanik[a], I. Svito[a], A. Saad[b], V. Fedotova[c], K. Czarnacka[d] and T.N. Koltunowicz[d,*]

[a]Belarusian State University, 220030, Minsk, Belarus
[b]Al Balqa Applied University, Physics Department, P.O. Box 4545, Amman 11953, Jordan
[c]Scientific-Practical Material Research Centre NAS of Belarus, 220040 Minsk, Belarus
[d]Lublin University of Technology, 20-618 Lublin, Poland

The present paper investigates the temperature/frequency dependences of admittance Z in the granular $Cu_x(SiO_2)_{1-x}$ nanocomposite films around the percolation threshold x_C in the temperature range of 4–300 K and frequencies of $20–10^6$ Hz. The behavior of low-frequency $ReZ(T)$ dependences displayed the predominance of electrons hopping between the closest Cu-based nanoparticles for the samples below the percolation threshold $x_C \approx 0.59$ and nearly metallic behaviour beyond the x_C. The high-frequency curves $ReZ(f)$ at temperatures $T > 10$ K for the samples with $x < x_C$ exhibited behavior close to $ReZ(f) \approx f^{-s}$ with $s \approx 1.0$ which is very similar to the known Mott law for electron hopping mechanism. For the samples beyond the percolation threshold ($x > x_C$), the frequency dependences of $ReZ(f)$ displayed inductive-like (not capacitive) behaviour with positive values of the phase shift angles.

DOI: 10.12693/APhysPolA.128.883
PACS: 84.37.+q, 72.80.Ga, 73.22.–f, 61.46.Df, 64.60.ah

1. Introduction

Composite materials consisting of metallic nanoparticles in a dielectric matrix are of main focus in material science research at present due to the presence of unresolved questions as far as understanding of their physical and practical concepts are concerned [1]. The first reason for this interest is associated with miniaturization of electronic devices and improvement their performance in the field of higher frequencies [2]. The second reason is connected with the possibility of changing resistivity of metal–dielectric composites in a wide region. The third reason is in incomplete understanding regarding their carrier transport mechanisms, in particular in observation of the negative capacitance effect in the impedance of composites when dimensions of metallic phase particles get close to nanosizes [3–5]. Understanding of some physical peculiarities in the electrical behaviour of metal–dielectric nancomposites depending on frequency, temperature and composition will allow to use some of them in future as miniaturized electrotechnical elements with tunable resistance, capacitance and inductivity.

The character of dc/ac carrier transport in nanocomposites containing metallic nanoparticles randomly distributed in the dielectric matrix should be strongly dependent on the composition of the material, and in particular, on the position of percolation threshold x_C. The latter is determined by volume of the metallic phase fraction x in a composite, ratio of metallic and dielectric phases conductances σ_m/σ_d, phase composition of nanoparticles and matrix and also some geometric parameters of metallic phases (dimensions of nanoparticles and their scattering by sizes, shape of nanoparticles and topology of their distribution in matrix, etc.) [6–9]. In accordance with the percolation theory for binary composites [10], at $x < x_C$ nanoparticles are randomly distributed in dielectric matrix, so that transport is mainly realized by tunneling of electrons from particle to particle through dielectric strata. In such state composite is on dielectric side of metal–insulator transition (MIT). However, since $x = x_C$ these particles become contact electrically to each other and beyond the percolation threshold $x > x_C$ form continuous current-conducting (percolating) routes for electrons that will shunt dielectric phase shifting composite on metallic side of MIT. Besides, for correct interpretation of the behavior of electric properties in many real composite materials we should also take into consideration the influence of the rest or specially introduced oxygen in a gas mixture during their preparation: the last one can result in the formation of oxide "shells" or precipitates at the interface between the metallic particles and dielectric matrix [3–5]. All this makes the structure of such composites more complicated than for the binary ones and can strongly change their properties.

As it was shown earlier in our works [3, 11], in the nanocomposite films containing FeCo-based nanoparticles embedded into dielectric matrix (alumina, PZT,

*corresponding author; e-mail: t.koltunowicz@pollub.pl

CaF_2) a maximal negative capacitance effect (prevailing of inductive-like contribution in admittance) was observed in the nanocomposites being on the dielectric side of MIT when composition was close to the percolative configuration. Note that these effects were studied only for the nanocomposites with magnetic metallic constituents (Fe, Co, Ni or their alloys) and never for the samples with non-magnetic highly-conductive metallic nanoparticles (like Cu or Al) in insulating matrix compatible with silicon planar microelectronic technology (SiO_2). Therefore, it was interesting to study the behaviour of admittance in the nanocomposites containing highly conductive nonmagnetic nanoparticles (like Cu) in SiO_2. Note that as regards the Cu–SiO_2 nanocomposites very few papers devoted to the study of electric properties, measured only in dc regime are found in the literature [12–17].

Therefore, the goal of this work was to elucidate the influence of metal-to-dielectric component ration in the composite films, consisting of Cu-based nanoparticles embedded into the dielectric (silica) matrix, on their structure and mechanisms of carrier transport based on the temperature/frequency dependences of impedance.

2. Experimental procedures

The $Cu_x(SiO_2)_{1-x}$ thin film samples with $0.36 < x < 0.70$ in the range of 3 to 5 μm thick were fabricated by ion-beam sputtering of the compound target with argon onto the motionless glass ceramic substrate. The deposition was carried out in a special vacuum chamber [16] evacuated down to 1×10^{-4} Pa and then filled with pure argon up to the total gas pressure of 9.6×10^{-2} Pa. The original configuration of the compound target enabled to prepare composite films with different metallic to dielectric fraction ratio in one technological process [9, 16].

The as-deposited granular films were subjected to the study of structure by scanning electron microscopy (SEM), X-ray diffraction (XRD) and the Raman spectroscopy (RS). For the XRD analysis the Bruker powder diffractometer working with Cu K_α radiation, a graphite monochromator on the diffracted beam and a scintillation counter with pulse-height discriminator were used. Diffraction patterns were taken over a wide angular range from $2\theta = 5°$ to 80°. For the SEM images a LEO 1455VP microscope was used. It was also equipped with a special microprobe X-ray analyzer with energy-dispersive Si:Li detector Rontec allowing to perform X-ray microanalysis for checking the samples' stoichiometry with accuracy of ≈1%. Thicknesses of the films were also measured on SEM with the accuracy ≈2–3% on the cleavages of the studied samples. μ-Raman spectra were taken at room temperature using a Nanofinder High End (Lotis TII, Belarus-Japan) confocal microscope based setup.

Comparing the SEM, XRD and RS data for different samples of the studied films allowed to draw some conclusions. The SEM images of the films with $x > 0.60$ contained Cu granules of approximately 100–200 nm dimensions (see inset in Fig. 1). This is also confirmed by

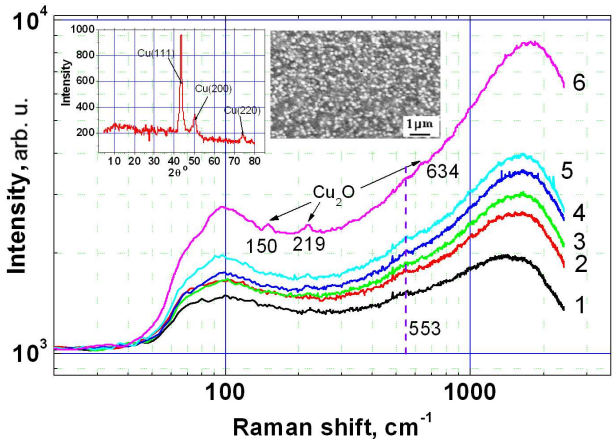

Fig. 1. RS spectra for the films with $x = 0.397$ (1), 0.510 (2), 0.607 (3), 0.628 (4), 0.658 (5) and 0.700 (6). Insets: X-ray diffraction pattern for the film with $x = 0.68$ (left) and SEM image for $x = 0.40$ (right).

the X-ray diffraction patterns in inset in Fig. 1. According to [18], the RS peaks (≈150, 219, 553, and 634 cm^{-1}) testify to the formation of Cu_2O phase in the films with $x > 0.60$ due to that the oxygen remains in the vacuum chamber during the deposition procedure.

The nanocomposite films for electric measurements were sputtered onto the glass-ceramic substrates and then cut into rectangular strips of 10 (length) × 2 (width) mm^2. Temperature dependences of admittance were measured in the temperature range 4–300 K using a closed-cycle cryogen-free cryostat system CFMS (Cryogenic Ltd., London), with Lakeshore Temperature Controller (Model 331) and PC based control system, which allowed either to change temperature with a rate of about 0.1–1 K/min in cooling/heating regimes or to stabilize temperature with the accuracy 0.005 K. The relative error of impedance measurements was less than 0.1%.

3. Results and discussion

In this section the results of impedance spectroscopy for $Cu_x(SiO_2)_{1-x}$ nanocomposite films for different temperatures T and compositions x are presented in Figs. 2 and 3. As it is commonly known [1, 2, 10], the carrier transport mechanisms of nanocomposites are strongly dependent on their position relative to the percolation threshold x_C. This value was specified as $x_C \approx 0.59 \pm 0.02$ by intersection of two curves presenting dependences of real parts of impedance ReZ on x in inset in Fig. 2 for the as-deposited (a) and annealed (b) samples measured at 295 K and the low frequency $f = 20$ Hz. As can be seen from the inset, the Re$Z(x)$ dependences have the reversal S-shaped view, which is characteristic of percolating systems [10], and the impedance is decreased by 5 orders of magnitude with the x increase in the region between 0.36 and 0.70.

The percolation threshold separates all the composites based on their composition on "dielectric" (for $x < x_C$) and "metallic" ($x > x_C$) that becomes apparent in

different behavior of impedance characteristics with temperature and frequency in Figs. 2, 3. As can be seen from curves 1–3 in Fig. 2, the Re$Z(T)$ dependences for $f = 20$ Hz show their activation ("dielectric") character for x less or close to the x_C value whereas for $x > 0.65$ they do not display activational character (curve 4 has nearly zero slope). The same behaviour was observed in [16] for temperature dependences of resistivity measured in the DC regime.

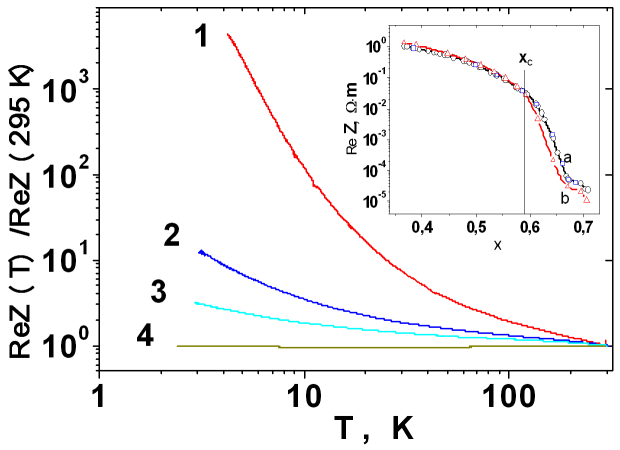

Fig. 2. Temperature dependences of normalized impedance Re$Z(T)$/ReZ(295 K) for the films with $x = 0.51$ (1), 0.60 (2), 0.63 (3) and 0.70 (4) measured at $f = 20$ Hz. Inset: ReZ vs. x for $Cu_x(SiO_2)_{1-x}$ nanocomposites in as-deposited (a) and annealed (b) states.

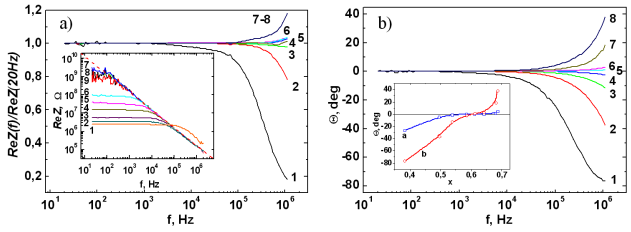

Fig. 3. Frequency dependences of normalized real part of impedance (a) and phase shift angle θ (b) for the films with $x = 0.38$ (1), 0.50 (2), 0.54 (3), 0.58 (4), 0.61 (5), 0.64 (6), 0.68 (7) and 0.69 (8). Inset in (a): Frequency dependence of ReZ(f) for the sample with $x = 0.38$ and temperatures $T = 260–300$ K (1), 220 K (2), 140 K (3), 80 K (4), 40 K (5), 20 K (6), 10 K (7), 8 K (8), 6 K (9). Dashed straight line in the inset (a) is extrapolation of high-frequency dependence of Re$Z(f)$. Inset (b): $\theta(x)$ dependence for 100 kHz (a) and 1 MHs (b).

Our experiments showed that the character of frequency dependences of ReZ and phase shift angle θ are strongly changed with composition and temperature. As follows from Fig. 3, for the samples with the activational behavior of Re$Z(T)$ in Fig. 2, i.e. at the concentrations of metallic phase $x > 0.59$, predominance of capacitive contribution in the imaginary part of impedance is observed (when $\theta < 0$ in Fig. 3b). For the films with "metallic" behavior for $x > 0.59$ the negative capacitance effect was observed that means delay of current as compared with the voltage applied and therefore prevailing of inductive contribution in the reactive impedance (with $\theta > 0$ in Fig. 3b).

Such behavior is observed in many metal–insulator composites where metallic granules in the dielectric matrix are nanosized and show hopping mechanism of carrier transport due to jumps of electrons between the neighboring metallic nanoparticles (see [3, 10, 16, 17]). In our case such mechanism is additionally confirmed by high-frequency Re$Z(f)$ dependences shown in inset (a) in Fig. 3. Actually, as can be seen from the comparison of these experimental curves with the straight dashed line, at high frequencies this dependence is very similar to the well-known Mott law [19] Re$Z(f) \sim f^{-s}$ with $s \approx 1.0$. In so doing, the frequency range, in which this law holds true, is expanded with the temperature lowering.

4. Conclusions

Our study of SEM images and XRD patterns of $Cu_x(SiO_2)_{1-x}$ nanocomposites with a wide range of metallic fraction content x showed that the as-deposited films displayed granular structure, where the copper granules are of about 100–200 nm dimensions around the percolation threshold $x_C \approx 0.59$. At the same time, the RS measurements indicate the presence of copper oxides on Cu nanoparticles which denotes possible limited oxidation of copper nanoparticles during deposition procedure in the oxygen remaining in vacuum chamber after its filling with Ar gas.

As follows from our study of temperature dependence of low-frequency impedance Re$Z(T)$ the investigated nanocomposite films with $x < 0.63$ are on the dielectric side of MIT and possess thermally activated hopping of electrons between the Cu nanoparticles by the Mott law as for dc measurements in [16, 17]. In doing so, in the dielectric regime nanocomposites display predominance of capacitive contribution in the reactive part of impedance whereas for $x > 0.68$ nanocomposites being on metallic side of MIT show prevailing inductive-like contribution in the reactive impedance Im$Z(f)$ in the form of negative capacitance effect with $\theta > 0$.

References

[1] Y. Imry, in: *Nanostructures and Mesoscopic Systems*, Eds. W.P. Kirk, M.A. Reed, Academic, New York 1992.

[2] G. Timp, *Nanotechnology*, Springer, New York 1999.

[3] P. Zhukowski, T.N. Kołtunowicz, P. Wegierek, J.A. Fedotova, A.K. Fedotov, A.V. Larkin, *Acta Phys. Pol. A* **120**, 43 (2011).

[4] T.N. Kołtunowicz, J.A. Fedotova, P. Zhukowski, A. Saad, A. Fedotov, J.V. Kasiuk, A.V. Larkin, *J. Phys. D Appl. Phys.* **46**, 125304 (2013).

[5] P. Żukowski, T. Kołtunowicz, J. Partyka, Yu.A. Fedotova, A.V. Larkin, *Vacuum* **83**, S275 (2009).

[6] R. Wood, *IEEE Trans. Magn.* **36**, 36 (2000).

[7] C. Baker, S.K. Hasanain, S. Ismat Shah, *J. Appl. Phys.* **96**, 6657 (2004).

[8] X. Huang, Z. Chen, *J. Cryst. Growth* **271**, 287 (2004).

[9] Yu.E. Kalinin, A.N. Remizov, A.V. Sitnikov, *Bull. Voronezh State Techn. Univ. Mater. Sci.* **N113**, 43 (2003).

[10] G. Grimmet *Percolation*, 2nd ed., Springer-Verlag, Berlin 1999.

[11] J.V. Kasiuk, J.A. Fedotova, M. Marszalek, A. Karczmarska, M. Mitura-Nowak, Yu.E. Kalinin, A.V. Sitnikov, *Phys. Solid State* **54**, 178 (2012).

[12] W. Chen, J.J. Lin, X.X. Zhang, H.K. Shin, J.S. Dyck, C. Uher, *Appl. Phys. Lett.* **81**, 523 (2002).

[13] X.X. Zhang, Chuncheng Wan, H. Liu, Z.Q. Li, Ping Sheng, J.J. Lin, *Phys. Rev. Lett.* **86**, 5562 (2001).

[14] K.V. Zapsis, A.S. Dzhumaliev, N.M. Ushakov, I.D. Kosobudski, *Techn. Phys. Lett.* **30**, 485 (2004).

[15] S. Banerjee, D. Chakravorty, *J. Appl. Phys.* **84**, 1149 (1998).

[16] A. Fedotov, I. Swito, A. Patryn, Y. Kalinin, A. Sitnikov, *Research Notes of the Faculty of Electronics and Computer Science of the Koszalin University of Technology* **4**, 29 (2012).

[17] I. Svito, A.K. Fedotov, T.N. Koltunowicz, P. Zhukowski, Y. Kalinin, A. Sitnikov, K. Czarnacka, A. Saad, *J. Alloys Comp.* **615**, S371 (2014).

[18] G. Niaura, *Electrochim. Acta* **45**, 3507 (2000).

[19] N.F. Mott, E.A. Davis, *Electron Processes in Non-crystalline Materials*, Clarendon Press, Oxford 1979.